ANALYSIS OF VARIABLE AMPLITUDE FATIGUE DATA OF A NOTCHED DETAIL MADE OF A PRESSURE VESSEL STEEL: COMPARISON OF DIFFERENT APPROACHES

António L.L. Silva, a.luis.l.silva@gmail.com
Engineering Department, School of Sciences and Technology, University of Trás-os-Montes e Alto Douro
Quinta de Prados, 5001-801 Vila Real, Portugal

Abílio M. P. de Jesus, ajesus@utad.pt
Engineering Department, School of Sciences and Technology, University of Trás-os-Montes e Alto Douro
Quinta de Prados, 5001-801 Vila Real, Portugal
UCVE, IDMEC – Pólo FEUP, Rua Dr. Roberto Frias, 4200-465 Porto, Portugal

Hélder F.S.G. Pereira, hfpereira@portugalmail.pt
UCVE, IDMEC – Pólo FEUP, Rua Dr. Roberto Frias, 4200-465 Porto, Portugal

Alfredo S. Ribeiro, aribeiro@utad.pt
Engineering Department, School of Sciences and Technology, University of Trás-os-Montes e Alto Douro
Quinta de Prados, 5001-801 Vila Real, Portugal
UCVE, IDMEC – Pólo FEUP, Rua Dr. Roberto Frias, 4200-465 Porto, Portugal

António A. Fernandes, aaf@fe.up.pt
Faculty of Engineering, University of Porto
Rua Dr. Roberto Frias, 4200-465 Porto, Portugal

Abstract. *This paper proposes a discussion on different approaches to assess variable amplitude fatigue data derived by authors for a notched detail made of a pressure vessel steel – the P355NL1 steel. The notched detail consists on a side notched rectangular plate with an elastic stress concentration factor of 2.17. This detail was fatigue tested under remote stress control, for variable amplitude loading. The variable amplitude loading consisted on block loading, namely sequences of variable amplitude blocks. The variable amplitude fatigue data of the detail is assessed using constant amplitude stress-life (S-N) and strain-life (ε-N) data, in the framework of a linear damage rule. Remote stress versus life data is available for the notched component in the form of S-N curves. Individual remote stress cycles are evaluated using the rainflow cycle counting method applied to the variable amplitude loading. A damage analysis is performed supported on a linear damage summation rule, applied together with information from constant amplitude S-N curves. Alternatively, individual remote stress ranges, resulting from the rainflow cycle counting, are transformed into local strain ranges, using a simplified notch stress-strain approach, such as the Neuber or Glinka analyses. This approach is often called as a classical local approach. Damage calculations are performed using strain-life data of the material, such as that correlated by Coffin-Manson with and without mean stress effects. Finally, a local cyclic elastoplastic analysis is performed for the notched component, using the remote stress-time history as input, resulting local stress-strain hysteresis loops. Simplified elastoplastic notch analysis is adopted, but key features observed on cyclic elastoplastic behaviour are taken into account. From this analysis, the cycle counting is straightforward, i.e., cycles result from closed hysteresis loops. The linear damage summation rule is applied, supported on strain-life data of the material, in particular de Coffin-Manson approach and the net effective strain range approach by DuQuesnay. All the approaches were implemented in macros, running on Excel spreadsheets. Distinct performances are verified for the proposed approaches.*

Keywords*: Notch Components, Fatigue Assessment, Variable Amplitude Loading, Local Approach, S-N Approach*

1. INTRODUCTION

Pressure vessel components invariably experience non-uniform loading histories during their service life, motivating research on material and component performance under variable amplitude loading, and the continual development of more reliable and accurate fatigue damage models.

Important pressure vessels design codes (ex. EN13445 standard (CEN, 2002)) propose procedures for fatigue analysis of variable amplitude loading that are supported by constant amplitude fatigue data and a linear damage summation rule, as proposed by Palmgren and Miner (Miner, 1945). This type of analysis neglects any load sequential effects that occur during the fatigue loading history, which is an important limitation. In fact, the linear summation rule does not consider the interaction effects between higher to lower stress levels or vice-versa. The linear damage rule also neglects the damage induced by any stress below the fatigue endurance limit.

Most of metallic materials and components exhibit more complex behaviours than modelled by the linear damage rule. However, and despite the limitations of the fatigue linear damage rule, the linear rule still is nowadays widely used for design purposes due to its simplicity.

It has been verified that some metallic materials and components exhibit highly nonlinear fatigue damage evolution with load dependency (Pereira *et al*., 2008a, 2008b, 2009a). The last two characteristics yield to nonlinear damage accumulation with load sequential effects. Thus, depending on load history, the Palmgren-Miner's rule can lead to inconsistent predictions, i.e., conservative or non conservative predictions.

Several attempts have been done to propose more reliable fatigue damage rules. Manson and Halford (1986), Fatemi and Yang (1998) and Schijve (2003) present comprehensive reviews about these fatigue damage models. However, the new propositions are often limited to very specific conditions (e.g. certain loading sequences, materials).

This paper proposes a discussion on different approaches to assess variable amplitude fatigue data, derived by authors, for a notched detail made of a pressure vessel steel – the P355NL1 steel (Pereira *et al*., 2008b, 2009b). The variable amplitude loading that will be analyzed in this paper consists on block loading, namely sequences of variable amplitude blocks, covering distinct stress R-ratios, stress ranges and spectrum sequences. The variable amplitude fatigue data of the detail is assessed using constant amplitude stress-life (S-N) data from the component and strain-life (ε-N) data from the material, in the framework of a linear damage summation rule (Miner, 1945). Remote stress *versus* life data available for the notched component, in the form of S-N curves, is applied in damage assessment, using the linear damage rule. To this respect, individual remote stress cycles are evaluated, applying the rainflow cycle counting method (ASTM, 1999), directly to the remote stress histories. Alternatively, individual remote stress ranges, resulting from the rainflow cycle counting, are transformed into local strain ranges, using a simplified notch stress-strain approach, such as the Neuber (1961) or Glinka (1985a, 1985b) analyses. This approach is often called as a classical local approach. Linear damage summations are performed using strain-life data of the material, such as that correlated by the classical Coffin-Manson model (Coffin, 1954; Manson, 1954) and the more recent DuQuesnay model (DuQuesnay, 2002; DuQuesnay *et al*., 1992, 1995; Lynn and DuQuesnay, 2002). The DuQuesnay model, being a strain based model, uses the concept of the net effective strain range as a damage parameter, to take fatigue into account as well as crack closure effects. Alternatively to the classical elastoplastic cyclic analysis, a local cyclic elastoplastic analysis is performed for the notched component, using the remote stress-time history as input, resulting physically admissible local stress-strain hysteresis loops. Again simplified elastoplastic notch analysis is adopted, but key features observed on cyclic elastoplastic behaviour are taking into account. From this analysis, cycles are counted based on closed hysteresis loops. Again, the linear damage summation rule is applied, supported on the strain-life models referred previously. All these approaches were implemented in the FLP (*Fatigue Life Prediction*) application, which consists on macros, running on Excel spreadsheets.

2. FATIGUE MODELLING

Basically, three main approaches have been proposed for fatigue assessment of structural components, namely the stress, strain and fracture mechanics based approaches. This paper proposes the application of the first two: the stress and strain based approaches, to assess variable amplitude data of a structural component. Typically, the referred approaches are based on constant amplitude experimental data, which requires a damage summation rule, to assess variable amplitude data. The linear damage rule, proposed by Miner (1945), which has been widely applied, assumes the following form:

$$D = \sum_i \frac{n_i}{N_{fi}} \leq 1 \tag{1}$$

where: n_i is the number of constant amplitude cycles, corresponding to a certain stress or strain range; N_{fi} is the number of cycles that would result in failure, for the same loading conditions of the applied n_i cycles. The failure occurs if D reaches the unity. The application of the damage rule requires, for spectrum loading, the use of a cycle counting technique, such as the rainflow method (ASTM, 1999). In the stress-based approach, the number of cycles to failure is directly correlated with a stress range that could be the nominal, the hotspot, the notch or other type of stress measures. Generally, this relation can be expressed as a power relation, as proposed by Basquin (1910):

$$\frac{\Delta\sigma}{2} = \sigma'_f \left(2N_f\right)^b \tag{2}$$

where: $\Delta\sigma$ is the stress range, σ'_f and b are constants and N_f is the number of cycles to failure. This relation is often used to correlate high cycle fatigue data of smooth specimens, where $\Delta\sigma$ represents the notch stress range. In those cases, σ'_f and b are named fatigue strength coefficient and exponent, respectively. Other alternative, but an equivalent representation of the stress-life relation, often used in design codes, is the following (CEN, 2002):

$$\Delta\sigma^m N_f = C \tag{3}$$

where: m and C are material constants.

In the framework of the strain-based approaches, the Coffin-Manson (Coffin, 1954; Manson, 1954) relation is very well established. This relation can be stated as follows:

$$\frac{\Delta\varepsilon}{2} = \frac{\sigma'_f}{E}\left(2N_f\right)^b + \varepsilon'_f\left(2N_f\right)^c \tag{4}$$

where: E is the Young modulus, ε'_f and c are the fatigue ductility coefficient and exponent, respectively, $\Delta\varepsilon$ is the total strain range. The other nomenclature of the previous equation is the same used in Eq. (2). This equation can be changed to account for mean stress effect, as suggested by Morrow (1965):

$$\frac{\Delta\varepsilon}{2} = \frac{\sigma'_f - \sigma_m}{E}\left(2N_f\right)^b + \varepsilon'_f\left(2N_f\right)^c \tag{5}$$

where: σ_m is the mean stress of the cycle.

Another alternative strain-life relation was proposed recently by DuQuesnay (2002). It takes into account crack closure effects using a net effective strain range parameter. The model proposed by DuQuesnay (2002) can be stated as follows:

$$\Delta\varepsilon^* = AN_f^{\ B} \tag{6}$$

where: $\Delta\varepsilon^*$ is the net effective strain range, A and B are material constants. The net effective strain range is defined as follows:

$$\Delta\varepsilon^* = \Delta\varepsilon_{eff} - \Delta\varepsilon_i \tag{7}$$

where: $\Delta\varepsilon_{eff}$ is the effective strain range and $\Delta\varepsilon_i$ is a material intrinsic fatigue limit, i.e., strain ranges bellow the intrinsic limit are not able to inflict damage. The effective strain range, $\Delta\varepsilon_{eff}$, corresponds to a fraction of the applied strain range, for which cracks are open. To define the effective strain range, a definition for the opening stress is required. DuQuesnay (2002) has been using the following empiric equation:

$$\sigma_{op} = \alpha\sigma_{max}\left[1 - \left(\sigma_{max}/\sigma_y\right)^2\right] + \beta\sigma_{min} \tag{8}$$

where: σ_{max} and σ_{min} are the maximum and minimum stress of the largest rainflow cycle in the spectrum (see Fig. 1), σ_y is the cyclic yield stress and α and β are material constants. An assumption of equal crack closure and crack opening stresses is assumed. Assuming that crack opening stresses occur at a region of linear elastic material behaviour, the corresponding opening strain can be estimated as follows:

$$\varepsilon_{op} = \varepsilon_{min} + \frac{\sigma_{op} - \sigma_{min}}{E} \tag{9}$$

Thus, the effective strain range can be defined as follows:

$$\begin{cases} \Delta\varepsilon_{eff} = \varepsilon_{max} - \varepsilon_{min} & if \quad \varepsilon_{min} > \varepsilon_{op} \\ \Delta\varepsilon_{eff} = \varepsilon_{max} - \varepsilon_{op} & if \quad \varepsilon_{min} < \varepsilon_{op} \end{cases} \tag{10}$$

The application of the previous local strain approaches requires the implementation of cyclic elastoplastic analysis, to derive the local strain histories. One possibility is to use simplified elastoplastic analysis such as the Neuber (1961) and Glinka (1985a, 1985b) analyses, applied together with the Ramberg-Osgood (Ramberg and Osgood, 1943) mathematical description of the cyclic curve of the material. Equations (11)-(12) can be used to estimate the local stress and strain ranges, provided that the nominal stress are provided, respectively using the Neuber and Glinka methods. In those equations, K' and n' are the cyclic strain hardening coefficient and exponent, K_t is the elastic stress concentration factor, $\Delta\sigma_l$ and $\Delta\varepsilon_l$ are the local stress and strain ranges and $\Delta\sigma_{nom}$ are the nominal stress range.

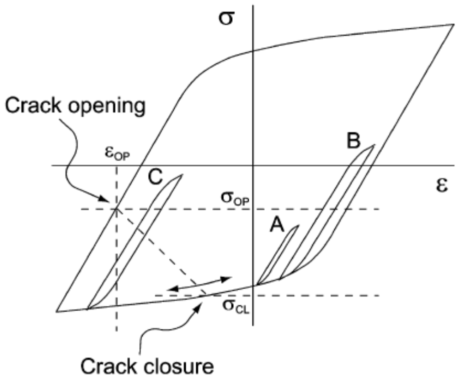

Figure 1. Crack opening *versus* crack closure behaviours (Lynn and DuQuesnay, 2002).

$$\begin{cases} \dfrac{\Delta\sigma_l^{\,2}}{E} + 2\Delta\sigma_l\left(\dfrac{\Delta\sigma_l}{2K'}\right)^{1/n'} = \dfrac{K_t^2\Delta\sigma_{nom}^2}{E} \\ \Delta\varepsilon_l = \dfrac{\Delta\sigma_l}{E} + 2\left(\dfrac{\Delta\sigma_l}{2K'}\right)^{1/n'} \end{cases} \tag{11}$$

$$\begin{cases} \dfrac{\Delta\sigma_l^{\,2}}{4E} + \dfrac{\Delta\sigma_l}{n'+1}\left(\dfrac{\Delta\sigma_l}{2K'}\right)^{1/n'} = \dfrac{K_t^2\Delta\sigma_{nom}^2}{4E} \\ \Delta\varepsilon_l = \dfrac{\Delta\sigma_l}{E} + 2\left(\dfrac{\Delta\sigma_l}{2K'}\right)^{1/n'} \end{cases} \tag{12}$$

3. THE FLP APPLICATION

The FLP application consists on macros, made in Visual Basic for Applications (VBA), running on Microsoft Excel spreadsheets, which makes it very accessible and easy to use. The FLP application is capable to implement the fatigue assessments according the formulae presented in Section 2. Additionally, the FLP code performs elastoplastic analysis according the Seeger-Heuler (Seeger and Heuler, 1980) equation and also includes the strain-life rule proposed by Topper, Smith and Watson (1970). These last two capabilities of the FLP application are not explored in this paper. Figure 2 illustrates the spreadsheet used to input the material constants, the nominal stress spectra and the desired assessment approach. Three main assessment approaches are possible to perform. The first one consists on performing a local elastoplastic analysis, transforming the nominal stress spectra into local stress-strain histories. Individual local stress-strain cycles are then counted based on closed stress-strain hysteresis loops. Then, the fatigue damage assessment can be performed using one of the proposed fatigue strain-life rules (Coffin-Manson, Morrow, DuQuesnay and TSW models). The second assessment approach consists on performing a cycle counting directly applied to the remote stress spectra, according the rainflow technique. Resulting individual remote stress cycles are transformed into local stress-strain cycles, using simplified elastoplastic analysis. Then, the fatigue strain-life rules are applied. Finally, the third assessment approach consists on performing a damage evaluation using directly the remote stress cycles, from the rainflow analysis, together with the S-N curves of the notch components. Ideally, several S-N curves should be supplied covering distinct stress ratios. Interpolation/extrapolation between stress R-ratios are performed by the application, when required.

Figure 3 illustrates some results in graphical form from the FLP application. For a given nominal stress spectra, the local stress-strain loops, the stress-time and strain-time histories are evaluated and plotted.

4. EXPERIMENTAL DATA

The P355NL1 steel, supplied in the form of 3140×2000×5.1 mm^3 plates, has been investigated by authors (Pereira *et al*., 2008a, 2008b, 2009a, 2009b), and is the basis for this study. This steel is intended for pressure vessel applications and is a normalized fine grain low alloy carbon steel. The mechanical properties of the material are given in Tab. 1 (Pereira *et al.*, 2008a, 2008b, 2009a, 2009b). Notched specimens made of P355NL1 steel, subjected to variable amplitude loading, are analysed in this paper. Figure 4 represents the geometry of the notched specimens. This component shows an elastic stress concentration factor, K_t, equal to 2.17, for tension/compression loading. Figure 5 gives the S-N curves obtained for the detail, under constant amplitude loading, covering three distinct stress ratios, R=0, R=0.15 and R=0.3 (Pereira *et al.*, 2008b). The notched component was submitted to variable amplitude fatigue tests, in particular variable amplitude block loading tests, under remote stress control. Figure 6 illustrates the variable amplitude block loading. Ten distinct variable amplitude blocks were used in the tests, namely:

- High-Low variable amplitude block loading with 100 individual stress cycles with R=0;
- Low-High variable amplitude block loading with 100 individual stress cycles with R=0;
- Low-High-Low variable amplitude block loading with 200 individual stress cycles with R=0;
- Random variable amplitude block loading with 100 individual stress cycles with R=0;
- Low-High variable amplitude block loading with 100 individual stress cycles with R=0.3;
- High-Low variable amplitude block loading with 100 individual stress cycles with R=0.3;
- Low-High-Low variable amplitude block loading with 200 individual stress cycles with R=0.3;
- Random variable amplitude block loading with 100 individual stress cycles with R=0.3;
- Random variable amplitude block loading with 100 individual stress cycles with R=0.0 and R=0.3;
- Random variable amplitude block loading with 100 individual stress cycles with R=0.0, R=0.3 and R=0.5.

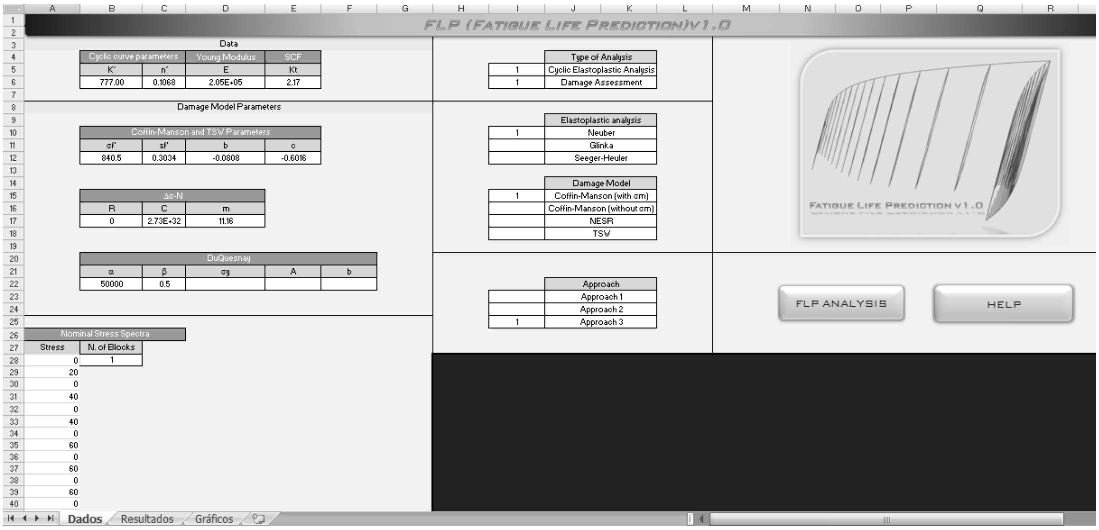

Figure 2. Input spreadsheet of the FLP application.

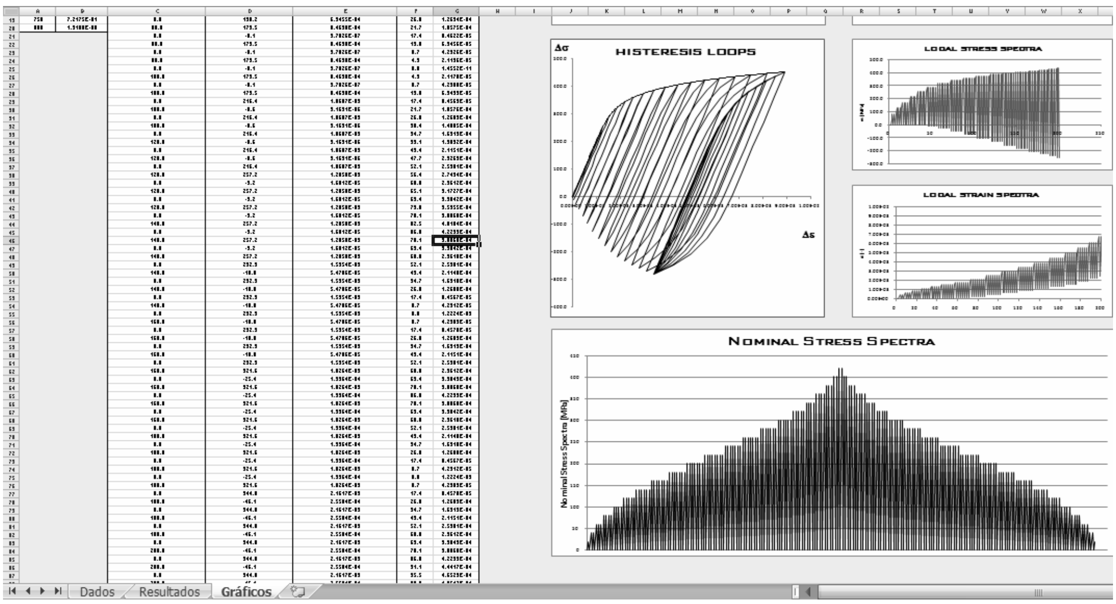

Figure 3. Graphical results from the FLP application.

Table 1. Mechanical properties of the P355NL1 steel (Pereira *et al*., 2008a, 2008b, 2009a, 2009b).

Ultimate tensile strength, σ_{UTS} [MPa]	568
Monotonic yield strength, $\sigma_{0.2}$ [MPa]	418
Cyclic yield strength, σ_y [MPa]	400
Young modulus, E [GPa]	205.2
Poisson's coefficient, ν	0.275
Cyclic hardening coefficient, K' [MPa]	777
Cyclic hardening exponent, n' [-]	0.1068
Fatigue strength coefficient, σ'_f [MPa]	840.5
Fatigue strength exponent, b [-]	-0.0808
Fatigue ductility coefficient, ε'_f [-]	0.3034
Fatigue ductility exponent, c [-]	-0.6016
Coefficient of the DuQuesnay's Model, A [MPa]	50000
Exponent of the DuQuesnay's Model, B	-0.5
Intrinsic fatigue limit, $E\Delta\varepsilon_i$ [MPa]	300
Parameter appearing in the definition of the closure stress, α	0.75
Parameter appearing in the definition of the closure stress, β	0

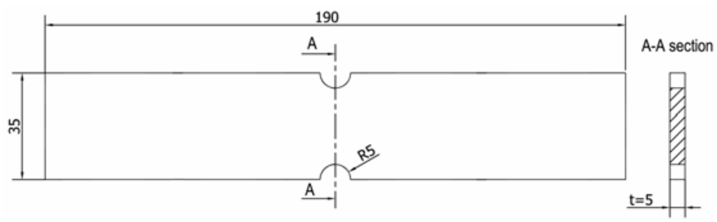

Figure 4. Geometry of the notched specimens (dimensions in mm).

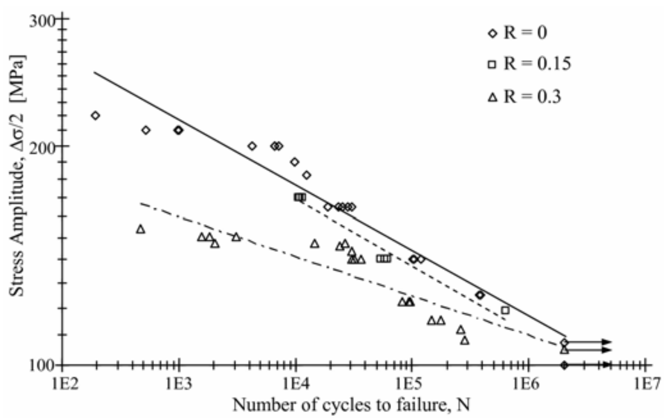

Figure 5. Constant amplitude S-N curves of the notched component (K_t=2.17) made of P355NL1 steel (Pereira *et al*., 2008b).

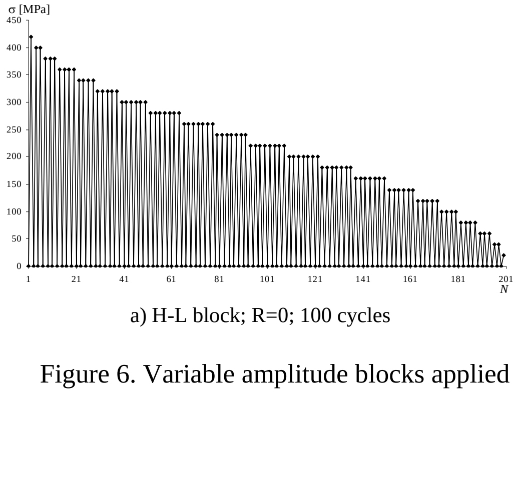

a) H-L block; R=0; 100 cycles

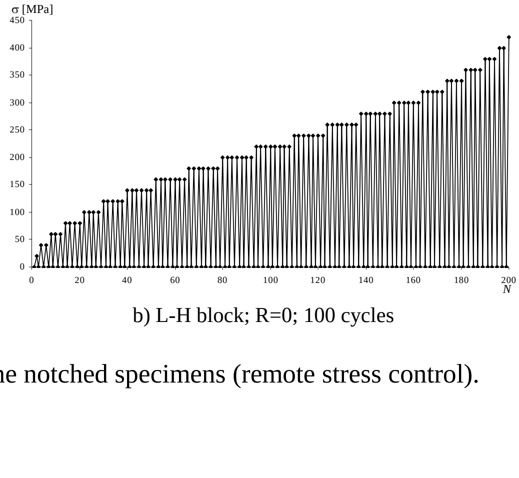

b) L-H block; R=0; 100 cycles

Figure 6. Variable amplitude blocks applied to the notched specimens (remote stress control).

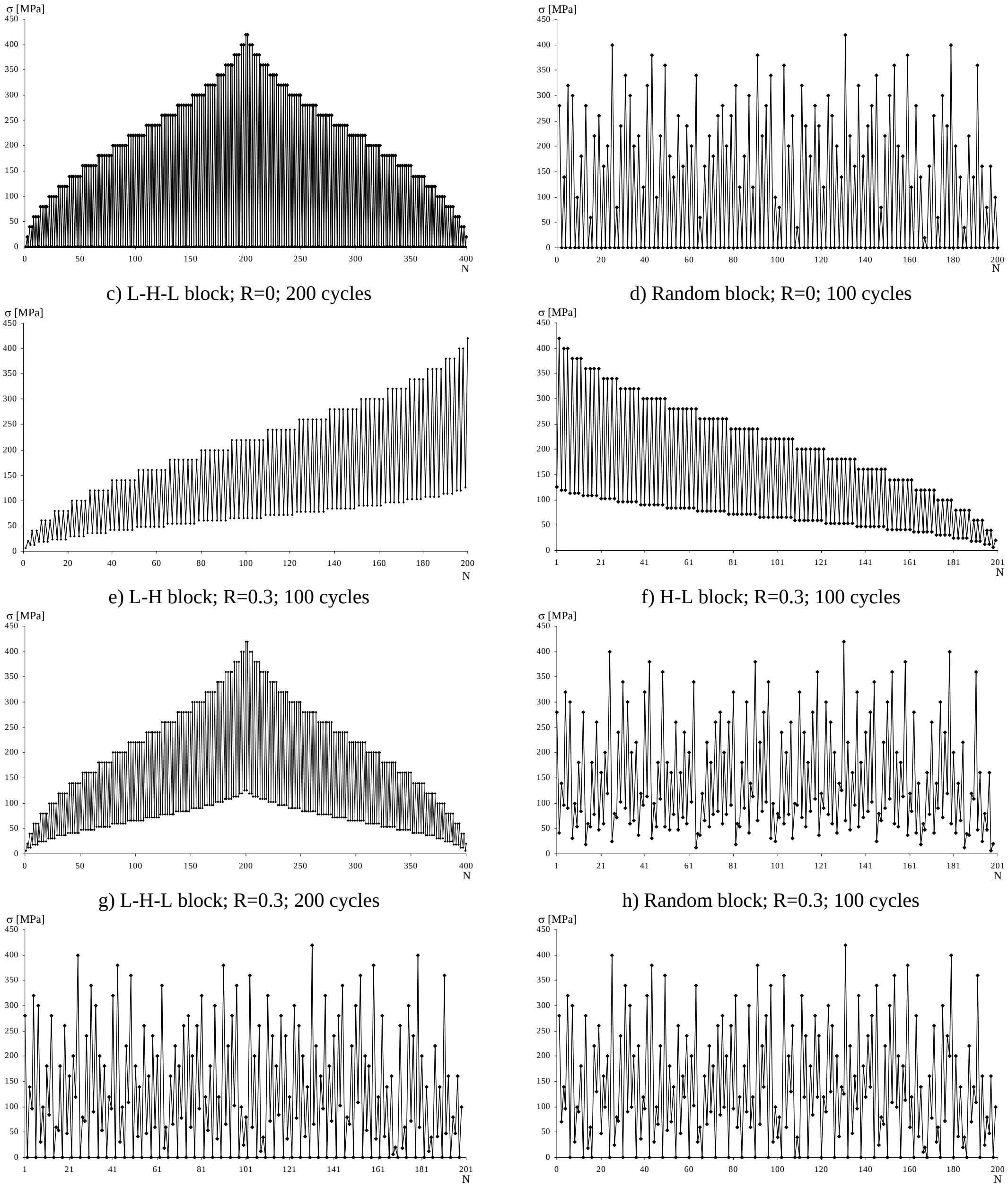

c) L-H-L block; R=0; 200 cycles

d) Random block; R=0; 100 cycles

e) L-H block; R=0.3; 100 cycles

f) H-L block; R=0.3; 100 cycles

g) L-H-L block; R=0.3; 200 cycles

h) Random block; R=0.3; 100 cycles

i) Random block; R=0+R=0.3; 100 cycles

j) Random block; R=0+R=0.3+R=0.5; 100 cycles

Figure 6. Variable amplitude blocks applied to the notched specimens (remote stress control) (continuation).

5. RESULTS AND DISCUSSION

Figure 7 gives the experimental fatigue lives as well as the predictions made according to several approaches available in the FLP application. A total of 13 predictions are proposed for each spectrum type, 12 based on local strain approaches and 1 based on the constant amplitude S-N curves of the notched component. Regarding the predictions based on the local strain approach, both Neuber and Glinka elastoplastic analyses were carried out (6 analyses for each elastoplastic rule). The local strain approaches used in the predictions were based on Coffin-Manson rule, with and without mean stress effects, and on DuQuesnay model. Finally, in order to apply the local strain approaches, the local (notch) stress-strain hysteresis cycles must be defined. This is done in two ways: (1) – the remote stress spectra is converted into local stress-strain spectra through the cyclic elastoplastic analysis, then closed hysteresis loops are counted; (2) – the rainflow cycle counting is applied to the remote stress spectra, then remote stress cycles are converted into local stress-strain cycles, using the elastoplastic analysis. The last approach to derive the local stress-strain cycles can be considered as a classical approach.

The analysis of the predictions reveals that the application of Neuber's rule yields always lower lives than obtained with the Glinka's rule, which is consistent with the fact that Neuber's rule overestimates the local strains, when compared to the Glinka's rule. The application of the Coffin-Manson's rule, with the mean stress effects, results always in lower lives, as expected. Predictions based on constant amplitude S-N curves are very satisfactory, since they fall always within the accuracy band of half/twice the observed experimental life. However, they require expensive experimental data, consisting on detail S-N curves for several distinct stress R-ratios. In an important number of cases, significant differences are found between predictions carried out based on the two alternative elastoplastic analysis procedures: (1) local elastoplastic analysis followed by cycle counting, (2) rainflow cycle counting followed by local elastoplastic analysis (classic approach). The elastoplastic analysis (1) led, in general, to higher life predictions. Some exceptions were observed, but in those cases, predictions are very close between the two elastoplastic analyses. The classical elastoplastic analysis (2) predicts physically inconsistent hysteresis loops since it does not account for the load sequence, plasticity memory effects and the monotonic loading from the virgin state of the material. The alternative elastoplastic approach seeks the reproduction of physically consistent hysteresis loops. However, this approach uses the cyclic curve to describe the branches of the hysteresis loops, which is a valid assumption only for Masing type materials. The P355NL1 steel presents some deviations from the Masing behaviour.

The DuQuesnay's model applied together the Glinka's rule, with a physically consistent elastoplastic analysis, gives predictions falling into the accuracy band of half/twice the observed life, with only few exceptions.

There is a significant scatter among the several predictions.

6. CONCLUSIONS

Variable amplitude fatigue data, available for a notched detail made of P355NL1 steel, was assessed in this paper, using several alternative procedures. The variable amplitude data resulted from fatigue tests consisting on variable amplitude block loading. The assessment procedures included local strain approaches and the S-N approach, all implemented in a software application – the FPL application. Supporting the local strain approaches, two alternative procedures were used to assess the local stress-strain hysteresis loops: (1) local elastoplastic stress-strain analysis followed by closed hysteresis loops counting; (2) remote cycle counting, using rainflow technique, followed by local elastoplastic stress-strain analysis. The second approach, despite being a classical approach, yields physically inadmissible stress-strain hysteresis loops. Despite being physically consistent, the first approach is based on formulae for elastoplastic analysis, making it suitable only for (quasi) Masing-type materials, not fully corresponding to the case of the P355NL1 steel. The analysis of the predictions revealed significant scatter among the several predictions. The S-N approach resulted predictions falling always within the accuracy range. Among the local strain approaches, the model proposed by DuQuesnay seemed to better reproduce the experimental data, despite few observed inconsistencies.

7. REFERENCES

ASTM - American Society for Testing and Materials, 1999, "E1049-85: Standard Practices for Cycle Counting in Fatigue Analysis", Vol. 03.01, West Conshohocken, PA, pp. 5-8.

Basquin, O.H., 1910, "The exponential law of endurance tests", Proceedings of ASTM, Vol. 10, No. II, pp. 625-630.

CEN - European Committee for Standardization, 2002, "EN 13445: Unfired Pressure Vessels", European Standard, Brussels.

Coffin, L.F., 1954, "A Study of the Effects of theC Thermal Stresses on a Ductile Metal", Translations of the ASME, Vol. 76, pp. 931-950.

DuQuesnay, D. L., 2002, "Applications of Overload Data to Fatigue Analysis and Testing," Application of Automation Technology in Fatigue and Fracture Testing and Analysis: Fourth Volume, ASTM STP 1411, A. A. Braun. P. C. McKeighan, A. M. Nicolson, and R. D. Lohr, Eds., American Society for Testing and Materials, West Conshohocken, PA, pp. 165-180.

DuQuesnay, D. L., MacDougall, C., Dabayeh, A., and Topper, T. H., 1995, "Notch Fatigue Behaviour as Influenced by Periodic Overloads," International Journal of Fatigue, Vol. 17, No. 2, pp. 91–99.

DuQuesnay, D.L., Topper, T.H. Yu, M.T. and Pompetzki, M.A., 1992, "The effective stress range as a mean stress parameter", International Journal of Fatigue, Vol. 14, No. 1, pp. 45-50.

Fatemi A., Yang L., 1998, "Cumulative fatigue damage and life prediction theories: a survey of the state of the art for homogeneous materials", International Journal of Fatigue, Vol. 20, No. 1, pp. 9-34.

Glinka, G., 1985a, "Energy Density Approach to Calculation of Inelastic Strain-Stress Near Notches and Cracks", Engineering Fracture Mechanics, Vol. 22, No. 3, pp. 485-508.

Glinka, G., 1985b, "Calculation of Inelastic Notch-Tip Strain-Stress Histories under Cyclic Loading", Engineering Fracture Mechanics, Vol. 22, No. 5, pp. 839-854.

Lynn, A.K., DuQuesnay, D.L., 2002, "Computer simulation of variable amplitude fatigue crack initiation behaviour using a new strain-based cumulative damage model", International Journal of Fatigue, Vol. 24, pp. 977-986.

Manson, S.S., 1954, "Behaviour of Materials under Conditions of Thermal Stress", NACA TN-2933, National Advisory Committee for Aeronautics.

Manson, S. S., Halford, G. R., 1986, "Re-examination of cumulative fatigue damage analysis - an engineering perspective", Engineering Fracture Mechanics, Vol. 25, pp. 538-571.

Miner, M.A., 1945, "Cumulative Damage in Fatigue", Journal of Applied Mechanics, Vol. 67, pp. A159-A169.

Morrow, J. D., 1965, "Cyclic plastic strain energy and fatigue of metals", Int. Friction, Damping and Cyclic Plasticity, ASTM, STP 378, pp. 45-87.

Neuber, H., 1961, "Theory of Stress Concentration for Shear-Strained Prismatic Bodies with Arbitrary Nonlinear Stress-Strain Law", Translations of the ASME, Journal of Applied Mechanics, Vol. 28, pp. 544-550.

Pereira, H.F.G.S., De Jesus, A.M.P., Fernandes, A.A. and Ribeiro, A.S, 2008a, "Analysis of Fatigue Damage under Block Loading in a Low Carbon Steel", Strain, Vol. 44, pp. 429-439

Pereira, H.F.G.S., De Jesus, A.M.P., Ribeiro, A.S. and Fernandes, A.A., 2008b, "Fatigue Damage Behavior of a Structural Component Made of P355NL1 Steel under Block Loading", Journal of Pressure Vessel Technology, Vol. 131, No. 2, pp. 021407(1)-021407(9).

Pereira, H.F.G.S., De Jesus, A.M.P., Fernandes, A.A. and Ribeiro, A.S, 2009a, "Cyclic and Fatigue Behavior of the P355NL1 Steel under Block Loading", Journal of Pressure Vessel Technology, Vol. 131, No. 2, pp. 021210(1)-021210(9).

Pereira, H.F.G.S., DuQuesnay, D.L., De Jesus, A.M.P., Ribeiro, Silva, A.L.L., 2009b, "Analysis of Variable Amplitude Fatigue Data of the P355NL1Steel Using the Effective Strain Damage Model", Journal of Pressure Vessel Technology, in press (DOI: 10.1115/1.3147986).

Ramberg, W., Osgood, W.R., 1943, "Description of stress-strain curves by three parameters", NACA Tech. Note No. 902.

Schijve, J., 2003, "Fatigue of structures and materials in the 20th century and the state of the art", Materials Science, Vol. 39, No. 3, pp. 307-333.

Seeger, T., Heuler, P., 1980, "Generalised application of Neuber's rule", Journal Testing Evaluation, Vol. 8, No. 4, pp. 199-204.

Smith, K. N., Watson, P., Topper, T. H., 1970, "A Stress-Strain Function for the Fatigue of Metals", Journal of Materials, Vol. 5, No. 4, pp. 767-778.

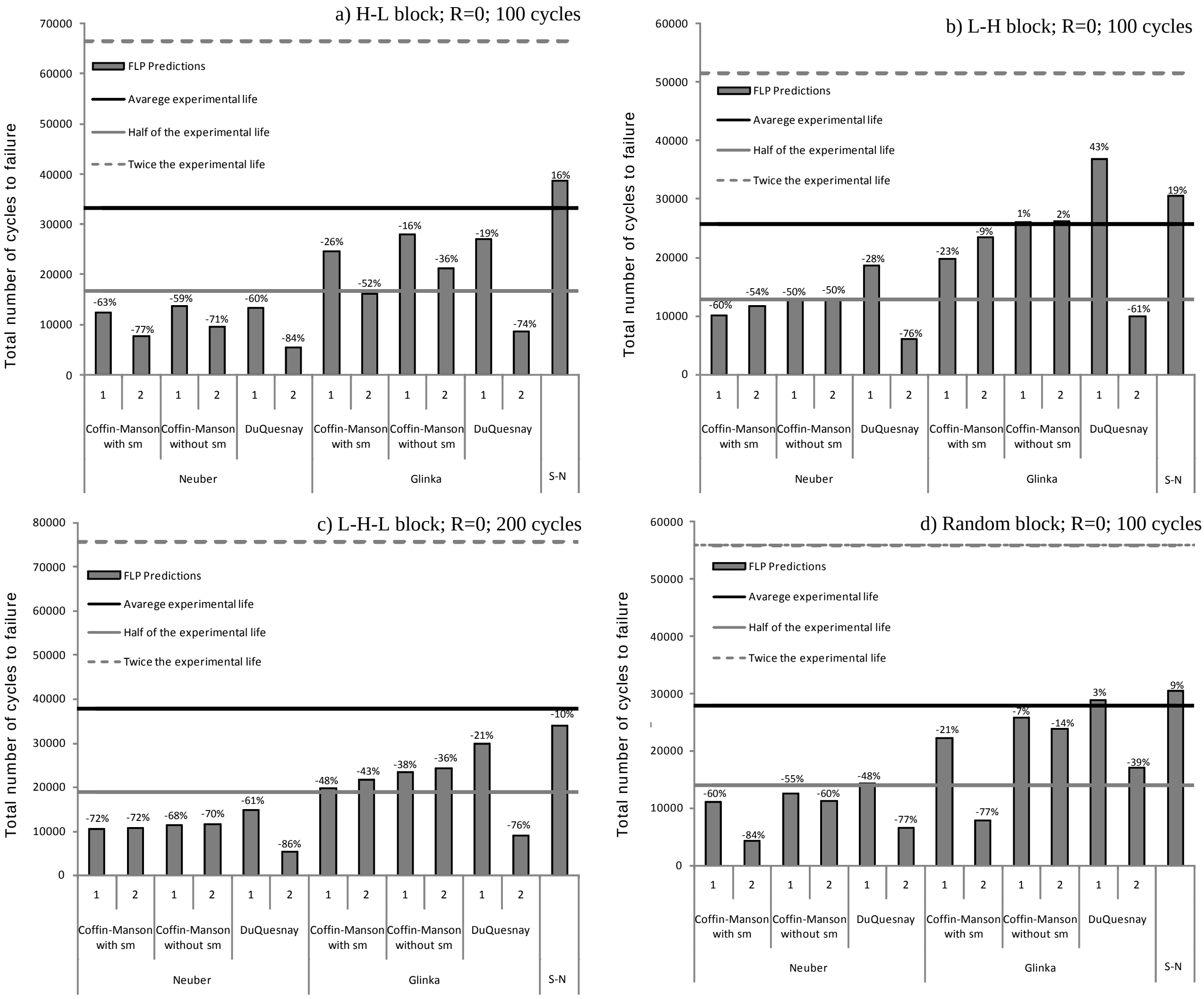

Figure 7. Fatigue life predictions for the variable amplitude block loading.

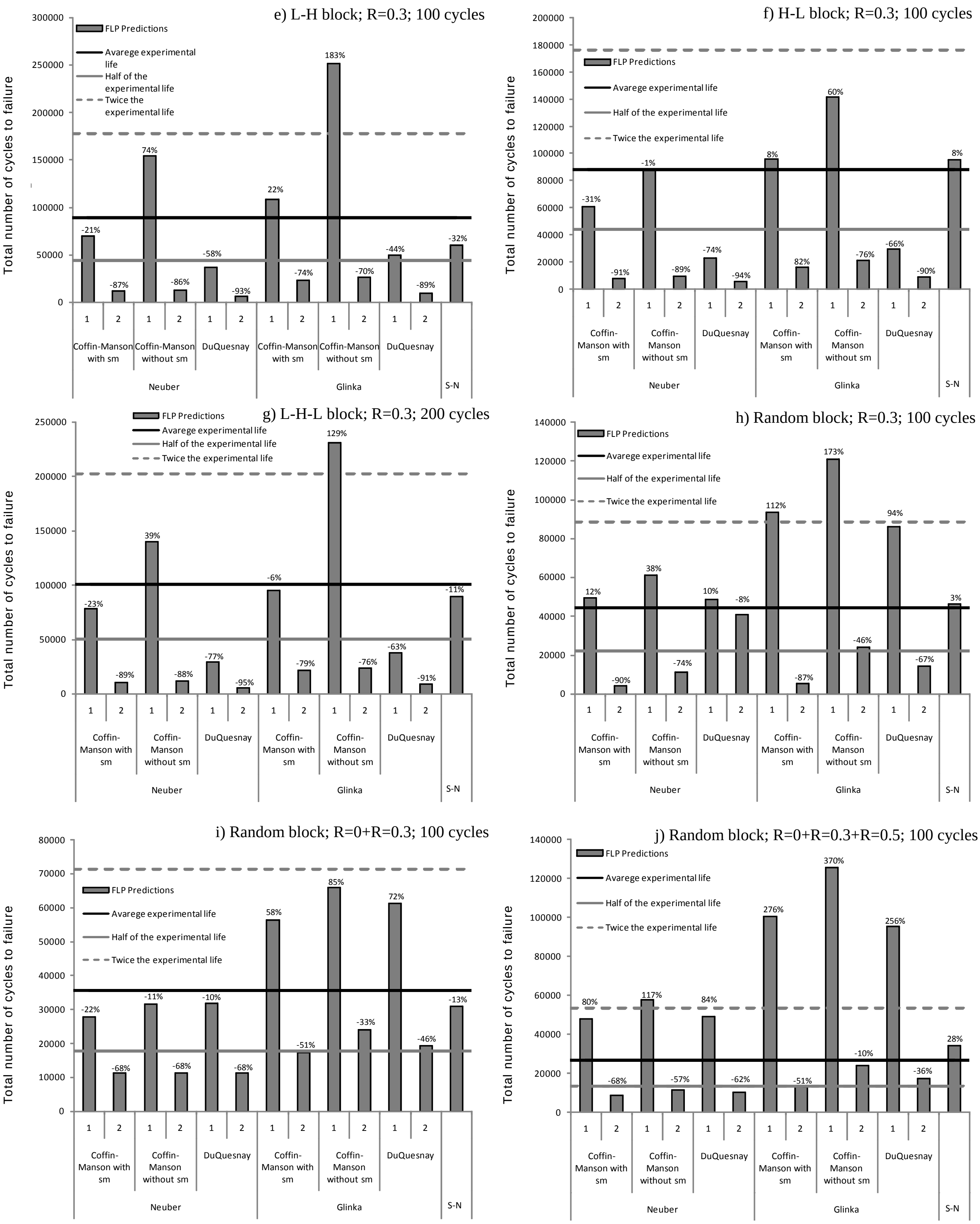

Figure 7. Fatigue life predictions for the variable amplitude block loading (continuation).

8. RESPONSIBILITY NOTICE

The authors are the only responsible for the printed material included in this paper.